COBEM 2025
28TH INTERNATIONAL CONGRESS OF MECHANICAL ENGINEERING

ABCM
Brazilian Society of Mechanical Sciences and Engineering
28th ABCM International Congress of Mechanical Engineering
November 09-11, 2025, Curitiba-PR, Brazil

COB-2025-2220
IOT SYSTEM FOR MONITORING THE PERFORMANCE OF A WATER SPRAY EVAPORATIVE COOLER

Vinicius Neves Macedo
Maurício Fernandes de Oliveira Assis
Helber Alencar de Vasconcelos
Andre Issao Sato
Universidade Federal do Oeste da Bahia, Av. Manuel Novais,1064, Bom Jesus da Lapa, BA
vinicius.m2420@ufob.edu.br
mauricio.a3347@ufob.edu.br
helber.v9431@ufob.edu.br
andre.sato@ufob.edu.br

Iug Lopes
Instituto Federal de Educação, Ciência e Tecnologia Baiano, BR 349, Km 14, Zona Rural, Bom Jesus da Lapa, Bahia
iug.lopes@ifbaiano.edu.br

Abstract. *Climate adversities at Brazil's semi-arid drive the search for solutions to mitigate its impacts. Bom Jesus da Lapa faces temperatures exceeding 40°C and low relative humidity, conditions that intensify thermal discomfort in urban spaces. To address this challenge, a water spray cooling system based on direct evaporative cooling was developed. To validate the system's efficiency, this study aimed to construct a data acquisition system alongside a robust sensor network around the cooling device to monitor the environment affected by water spray, collecting data on temperature, humidity, wind speed/direction, and spray pressure. This research proposes a high-density sensory measurement system capable of validating the cooling device as a solution for urban thermal comfort. The work details the designed IoT monitoring system, emphasizing instrumentation and precise recording of sensory data. The instrumentation integrated 25 SHT31 temperature and humidity sensors (24 radially positioned around the system and 1 external reference sensor), a cup anemometer, a wind direction indicator, and a pressure transmitter. Data acquisition was ensured by two microcontrollers: an Arduino UNO, responsible for reading the pressure sensor, and an ESP32, tasked with communicating with digital/anemometric sensors and Wi-Fi transmission. Both were integrated into dedicated printed circuit boards. Management of the 25 SHT31 sensors was managed by two I²C multiplexers (TCA9548A). The SHT31 sensors were protected against moisture and solar radiation, with calibrations ensuring data reliability (±0.2°C for temperature and ±2% for humidity). Data, collected every 10 seconds on the Arduino and 3 seconds on the ESP32, were transmitted via HTTP GET to a spreadsheet using Google Apps Script. The system demonstrated efficiency in data organization and transmission, even under direct sunlight and ambient temperatures exceeding 45°C. The monitoring system stood out for its low cost (due to dual addressing of digital sensors) and scalability (enabled by I²C multiplexers).*

Keywords: *Data Acquisition, Internet of Things, Thermal Comfort.*

1. INTRODUCTION

The western region of Bahia is characterized by a hot semi-arid climate, with a dry season that extends from 6 to 8 months and monthly average temperatures above 18 °C throughout the year (IBGE, 2002). Albuquerque e Silva (2008) state that the average annual temperatures in the semi-arid region are high, ranging between 23 °C and 27 °C, while the relative humidity is low, with annual average values around 50%. These severe climatic conditions intensify thermal discomfort in outdoor urban environments, impacting quality of life and the use of public spaces.

An alternative to promote thermal comfort in open spaces under the adverse urban semi-arid climate is evaporative cooling. According to Camargo (2003), this method is effective in hot and dry environments. In addition to lowering high temperatures, it increases the relative humidity of the air, improving local thermal conditions. However, an accurate assessment of the efficiency of these systems under real operating conditions, considering the dynamics of environmental variables (temperature, humidity, wind), requires robust and detailed monitoring systems.

Evaluating the effectiveness of such cooling systems demands precise environmental data collection with high spatial and temporal resolution. Conventional monitoring systems may not adequately capture the localized variability of spray effects, especially under the influence of factors such as wind direction and speed. The Internet of Things (IoT) offers powerful tools to develop low-cost, high-quality distributed data acquisition systems with real-time transmission capabilities that can be applied in various applications (Sunny et al., 2020).

In this context, this study details the development, implementation, and validation of a high-density sensory IoT monitoring system, specifically designed to evaluate the efficiency of a water spray cooling prototype in Bom Jesus da Lapa - BA. The main objective was to build and validate a data acquisition system capable of accurately and reliably recording variations in temperature, humidity, wind speed and direction, and spray pressure around the cooler, allowing for a detailed performance analysis under real conditions and validating the monitoring tool itself as an effective and scalable solution for studies analyzing environmental variables in open spaces.

2. EXPERIMENTAL PROCEDURE

This section briefly describes the spray cooling prototype used as a case study. Additionally, it details the development and construction of the IoT-based climate monitoring system, as well as the calibration procedures for the sensors employed.

2.1 SPRAY COOLING PROTOTYPE

The cooling system evaluated in this study consists of a portable prototype in the form of a movable post, as illustrated in Figure 1. Its construction employed PVC pipes, spray nozzles with 0.6 mm diameter orifices, a diaphragm pump operating at 12 V and 690 kPa, and a reservoir with a capacity of 50 liters of water, in addition to other components detailed in Figure 1.

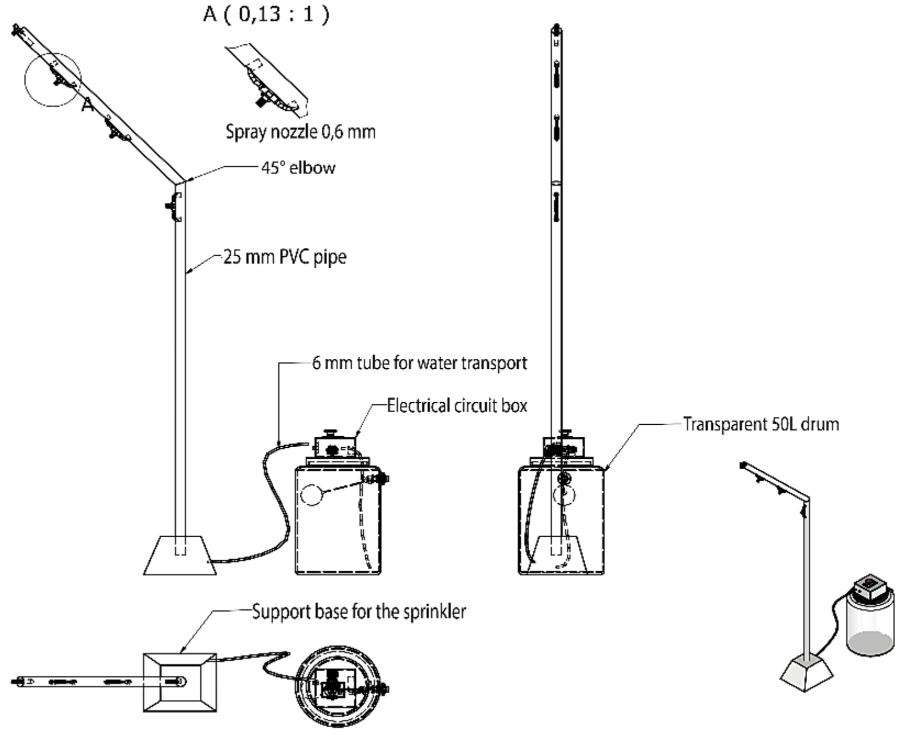

Figure 1. Cooling system model, from Authors (2025)

2.2 IOT MONITORING SYSTEM ARCHITECTURE

The data acquisition system used for monitoring was composed of a sensor network managed by microcontrollers, designed to collect information in outdoor environments, specifically regarding solar radiation and water spraying. The core of the system consists of two custom printed circuit boards (PCBs) (Figure 2 and Figure 3), which integrate the microcontrollers, I²C multiplexers, signal converter modules (current to voltage), connectors for various sensors, and power terminals, with jumpers responsible for sharing power supply voltage levels between boards, UART serial communication, and transmission of signals from the HW-685 converters.

Two distinct microcontrollers were used: an Arduino UNO, dedicated exclusively to reading the pressure transmitter, and an ESP32, responsible for communication with the SHT31 digital sensors via the I²C protocol, for reading the voltage signals (converted from current by the HW-685 modules) from the anemometer and the wind direction sensor, and for transmitting the collected data via Wi-Fi network.

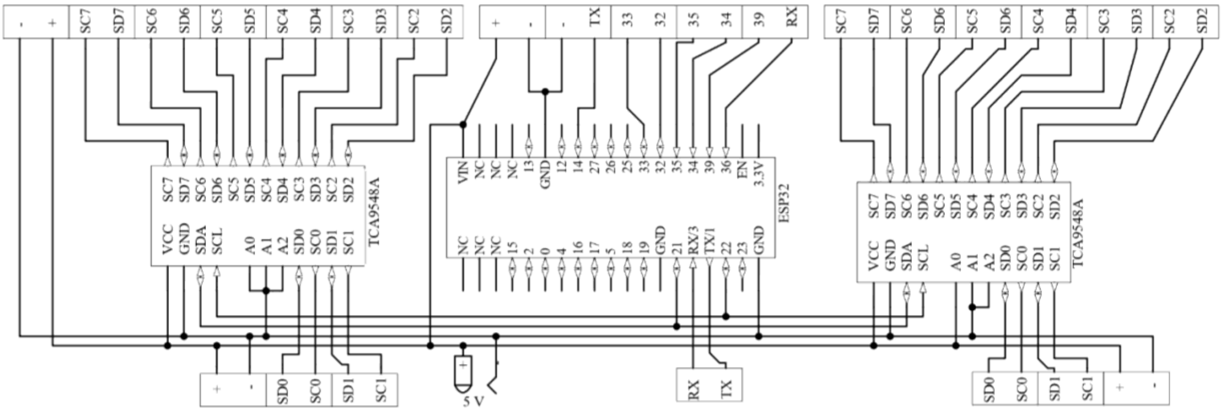

Figure 2. ESP32 PCB schematic, from Authors (2025)

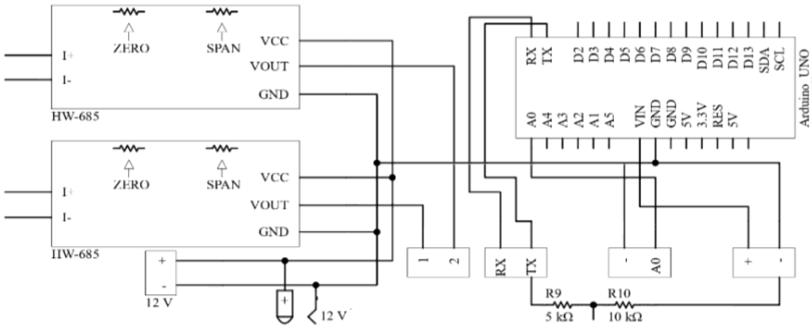

Figure 3. Schematic of the PCB with Arduino UNO, from Authors (2025)

Given the large number of SHT31 sensors (25 units) and the sensor's intrinsic limitation to only two selectable I²C addresses (0x44 and 0x45), the use of I²C multiplexers became necessary. Two TCA9548A integrated circuits were employed, connected to the same I²C bus of the ESP32. As described by (Deshmukh et al., 2023), the TCA9548A allows overcoming the limitation of identical I²C addresses on the same bus by providing eight independent communication channels, each activated by configuring bits in its control register via the I²C interface with the microcontroller. To differentiate the two multiplexers on the bus, their addresses were physically configured: one was set to 0x71 and the other to 0x70, using different combinations of connections of the address pins A0, A1, and A2 to GND or VIN, as specified by the manufacturer (Instruments, 2021). This architecture enabled individualized communication with all 25 SHT31 sensors from the ESP32.

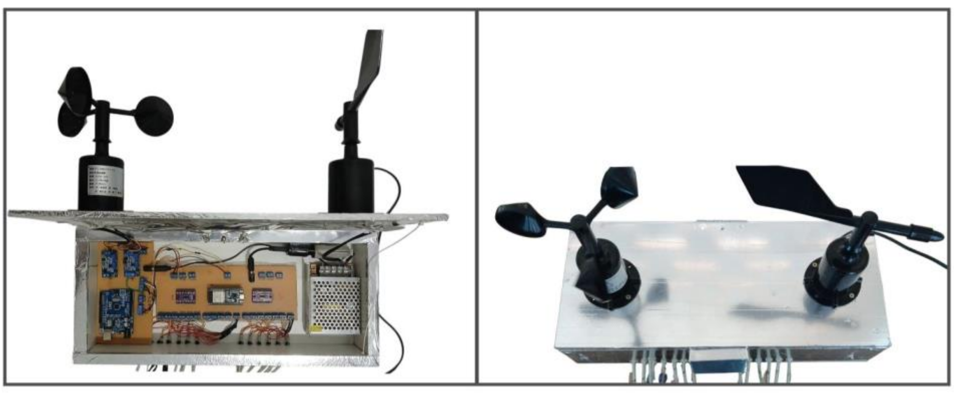

Figure 4. Circuits assembly (left) and external view (right), from Authors (2025)

The PCBs, with all components properly soldered, were housed in a protective enclosure with a lid (Figure 4a). The cup anemometer and wind direction sensor were mounted on top of this lid (Figure 4b). Inside, the enclosure contains a 5 V power supply and a shielded 12 V power supply. External connectors were installed on the box to facilitate the connection and disconnection of the external sensor cables. The PCB associated with the ESP32 (Figure 2) was powered with 5 V, which also supplies the ESP32 itself, the TCA9548A multiplexers, and the SHT31 sensors connected to it. The 12 V supply was used to power the HW-685 converter modules, the Arduino UNO R3 (Figure 3), the pressure transmitter, and the anemometric sensors.

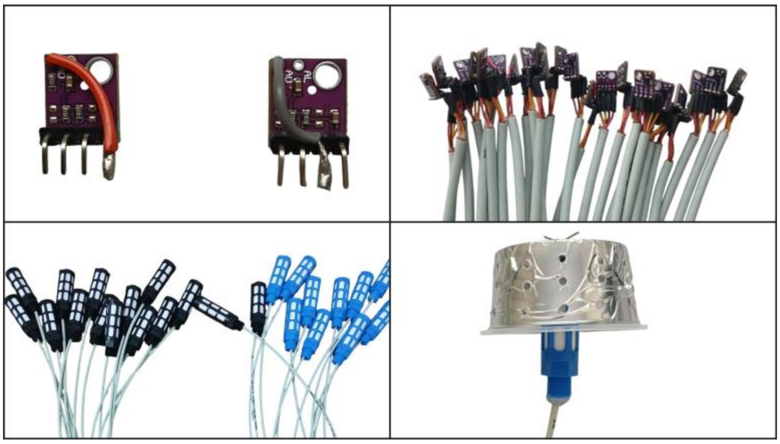

Figure 5. SHT31 sensors after address configuration (top left), with cables soldered (top right), with enclosure (bottom left), and solar radiation shield (bottom right), from Authors (2025)

Following the manufacturer's specifications (Sensirion, 2022), the I²C address configuration of each SHT31 sensor was physically conducted by connecting the sensor's ADDRESS pin to either the power supply (VIN) or ground (GND), avoiding leaving it floating. In this way, 13 sensors were configured with address 0x45 (ADDRESS pin connected to VIN) and the remaining 12 with address 0x44 (ADDRESS pin connected to GND), as illustrated in Figure 5a, which shows the sensors after address definition and cable soldering. To protect the sensors from adverse environmental conditions, each SHT31 was encapsulated in a sintered polyethylene protective enclosure, water-resistant (Figure 5c), similar to the one described by (Cornei; Fosalau; Cornei, 2024). Additionally, solar radiation shields were constructed using plastic cups (Figure 5d), based on the design proposed by (Da Cunha, 2015).

2.3 DATA ACQUISITION AND TRANSMISSION PROCEDURE

Data collection and logging were managed by three separate codes: a C++ program for the ESP32 microcontroller, another C++ program for the Arduino UNO, and a JavaScript script executed in Google Apps Script. The latter was responsible for receiving and storing the transmitted data in a Google Sheets spreadsheet. The developed source codes are publicly available in the repository: https://github.com/vinicius91050425/Esp32_aquisicao/tree/main. Figure 6 illustrates the overall flowchart of the data acquisition and transmission process.

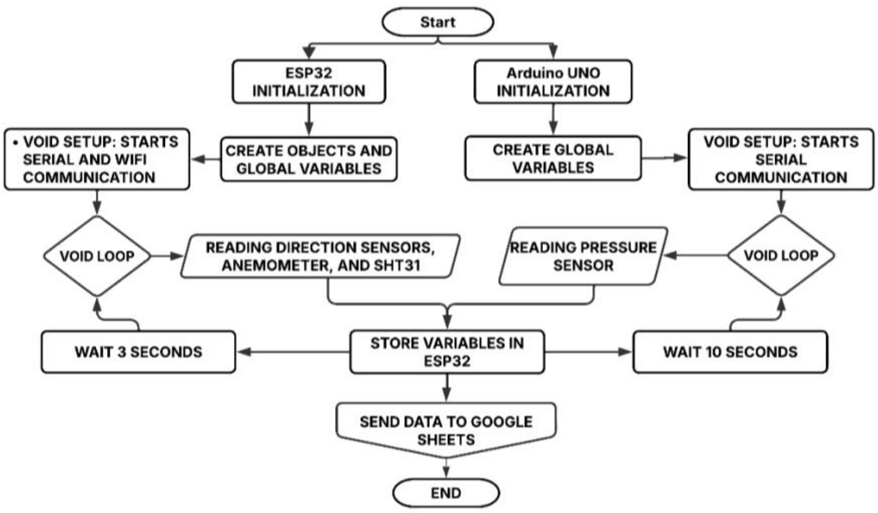

Figure 6. Flowchart of data collection and recording, from Authors (2025)

The Arduino UNO was specifically programmed to read the analog signal coming from the pressure transmitter. This sensor operates with an output voltage that varies linearly from 0.5 V to 4.5 V, corresponding to a pressure range from 0 MPa to 1.03 MPa. The Arduino's 10-bit analog-to-digital converter (ADC) converts this voltage range into digital values between 102 (for 0.5 V) and 920 (for 4.5 V). The conversion from the raw digital reading (ADC) to the corresponding pressure in psi (P) was implemented in the code using linear interpolation described in Eq. (1):

$$P = \left(\frac{ADC - offset}{fullScale - offset}\right) \cdot 150, \tag{1}$$

In Eq. (1), ADC is the digital value read by the Arduino, offset (102) is the digital value corresponding to the minimum pressure (0 MPa), fullScale (920) is the digital value for the maximum pressure (1.03 MPa), and 150 is the pressure range amplitude in psi. The calculated pressure value P (in psi) is subsequently transmitted by the Arduino to the ESP32 via serial communication (UART), using GPIO36 (ESP32 RX2 connected to Arduino TX) and GPIO14 (ESP32 TX2 connected to Arduino RX) pins.

The calibration of the HW-685 modules (4-20 mA current to 0-3.3 V voltage converters) was performed by adjusting the offset (zero) and span (gain) based on the wind direction sensor scale. For the anemometer, which also provides a current signal proportional to wind speed, the corresponding HW-685 module converts this signal into voltage. The ESP32 reads this voltage through its 12-bit analog-to-digital converter (ADC) (digital range 0–4095). The resulting digital value (ADC) is then converted to wind speed (V) in m/s, according to the linear relationship presented in Eq. (2):

$$V = \frac{ADC \cdot 30}{4095}, \tag{2}$$

In this linear relationship, ADC is the digital value read by the ESP32, 4095 is the maximum reading value of the 12-bit ADC, and 30 represents the maximum wind speed in m/s corresponding to the maximum ADC reading, according to the sensor and converter's operating range and calibration.

The wind direction determination was performed by mapping specific voltage ranges (or the corresponding digital values read by the ESP32 ADC after conversion by the HW-685) to each of the eight main geographic directions (N, NE, E, SE, S, SW, W, NW). Calibration established that each direction change resulted in an increment or decrement of 0.46 V in the output signal voltage of the direction sensor, allowing the identification of the predominant direction in the ESP32 code.

As mentioned in Section 2.2, the readings from the 25 SHT31 sensors were managed using two I²C multiplexers TCA9548A (addresses 0x71 and 0x70) connected to the ESP32. The sensors were logically grouped: those with index i from 1 to 13 were connected to the multiplexer 0x71, while sensors with index i from 14 to 25 were connected to the multiplexer 0x70. To select the appropriate channel in each multiplexer and communicate with a specific sensor with index i, the following mapping logics were implemented in the ESP32 code:

For sensors i from 1 to 13 (connected to Mux 0x71):

$$Channel = \frac{i-2}{2} + 2, \tag{3}$$

For sensors i from 14 to 25 (connected to Mux 0x70):

$$Channel = \frac{i-13}{2} + 2, \tag{4}$$

In Eqs. (3) and (4), i represents the sensor index varying from 1 to 25. The division operation should be interpreted as integer division, discarding the remainder. The implemented logic—subtracting an offset (2 for the first group, 13 for the second), dividing by 2, and adding 2—maps the sequential sensor index i to the corresponding physical channel number in the appropriate multiplexer. This mapping considers the alternating distribution of sensors with I²C addresses 0x44 and 0x45 among the available channels on the two multiplexers. To avoid conflicts on the I²C bus, the code was programmed to disable all channels on both multiplexers before enabling the specific channel for reading a sensor, thus ensuring individualized access, and preventing interference.

The transmission of the collected data to the cloud began with the ESP32 connecting to a pre-configured Wi-Fi network using the SSID and password defined in the code, with automatic reconnection attempts in case of failure. Once connected, the ESP32 sent data from all sensors (temperature, humidity, pressure, wind speed, and direction) to a Google Sheets spreadsheet via HTTP GET requests directed to a web app published through Google Apps Script. The request URL contained the data formatted as key=value pairs in the query string parameters. The script in Google Apps Script processed these parameters, extracting the variable values and recording them, along with date and time, into specific columns of a new row in the designated spreadsheet. This process, repeated at each complete measurement cycle, ensured traceability and structured organization of the data for subsequent analysis.

2.4 SENSOR CALIBRATION

Specific calibration procedures were adopted for each type of sensor, considering their characteristics and operating environment. The pressure transmitter (±1.5 psi) was calibrated by comparing its readings with those of a reference manometer (±1.5%) under controlled conditions. The SHT31 temperature and humidity sensors, which have an accuracy of ±0.2°C for temperature and ±2% for relative humidity, were validated in a thermally insulated environment using a thermo-hygrometer (with temperature accuracy of ±0.2°C and humidity ±2.5%) calibrated as a reference standard. The cup anemometer (±0.2% + 0.03 m/s) was calibrated by direct comparison with a reference digital anemometer (±5% + 0.5 m/s) in a wind tunnel. For the pressure transmitter and the anemometer, the calibration procedures involved multiple measurements performed in cycles of increasing (advance) and decreasing (return) the measured quantity to evaluate hysteresis.

The calibration of the pressure transmitter, connected to the Arduino, was conducted at the Mechanical Engineering Laboratory of the Universidade Federal do Oeste da Bahia (UFOB). A standard manometer installed in a compressed air treatment unit was used as a reference. The transmitter was pneumatically connected to the system through a ball valve and a 6 mm hose. The procedure consisted of varying the applied pressure, recording 12 measurement points during the gradual increase of pressure (advance) up to 55 psi (value indicated by the reference manometer) and another 12 points during the gradual pressure decrease (return).

For validation of the SHT31 sensors, all 25 sensors, connected to their respective acquisition electronics, were arranged inside an expanded polystyrene box to create a thermally stable and insulated environment. The box was then closed and sealed with adhesive tape to minimize air exchange with the external environment. A small side opening allowed the insertion of the probe of a calibrated thermo-hygrometer used as a reference. After a thermal stabilization period of 10 minutes, the data collection process began and lasted for 120 minutes. During this period, temperature, and humidity readings from all 25 SHT31 sensors and the reference thermo-hygrometer were recorded simultaneously every 8 minutes, allowing comparison of the SHT31 sensor readings with the reference standard and verification of their compliance with accuracy specifications.

The calibration of the cup anemometer was performed in a wind tunnel by comparing its readings with those of a reference digital anemometer. Both instruments were positioned close to each other and aligned with the airflow in the test section of the tunnel. Before starting the calibration, the anemometer was run for 5 minutes to avoid the effects of large temperature variations that could affect the friction of bearings and bushings of the anemometer. Furthermore, the calibration was intended to be performed at airflow speeds ranging from 4.0 to 16 m/s; however, due to the wind tunnel speed limitation, this range was from 0.6 to 6 m/s (MEASNET, 2020). Thus, the calibration procedure involved controlling variation of the air speed in the tunnel by adjusting the fan motor frequency, collecting 46 measurement points during the speed increase (advance) and another 46 points during speed decrease (return), covering the operational range of interest.

2.5 FIELD EXPERIMENTAL SETUP

Field experiment was conducted in the courtyard of the Multidisciplinary Center at the Federal University of Western Bahia (UFOB), Bom Jesus da Lapa campus. The spray cooling prototype was installed at the center of the designated experimental area. The data acquisition system (containing the PCIs, power supplies, and anemometric sensors) was mounted on a stand at a height of 2.5 meters above ground level, adjacent to the cooler, to protect it from the sprayed water mist.

To connect the SHT31 sensors distributed in the field to the central acquisition system, a network of 4-wire shielded cables equipped with quick connectors was designed and implemented. Twenty-four of these sensors, intended for measuring temperature and relative humidity, were positioned radially around the spray point, as schematically shown in Figure 7. A twenty-fifth SHT31 sensor (identified as sensor index 1) was installed approximately 10 meters away from the sprayer, functioning as a reference for environmental conditions not directly influenced by the mist. The pressure transmitter was installed on the water supply line of the sprayer, near its base, to monitor the operating pressure. All 25 SHT31 sensors, already connected to the cables and properly protected as described in Section 2.2, were fixed on stands at a height of 1.65 m from the ground, in distinct radial positions relative to the sprayer as shown in Figure 8.

The capability to configure the SHT31 sensors with two distinct I²C addresses (0x44 and 0x45) allowed optimization of the wiring, enabling the connection of two sensors with different addresses to a single 4-wire cable coming from the acquisition system, sharing the power lines, GND, SDA, and SCL through the multiplexer. Figure 7 schematically illustrates this radial arrangement, where the lines indicate the distribution of cables and sensors.

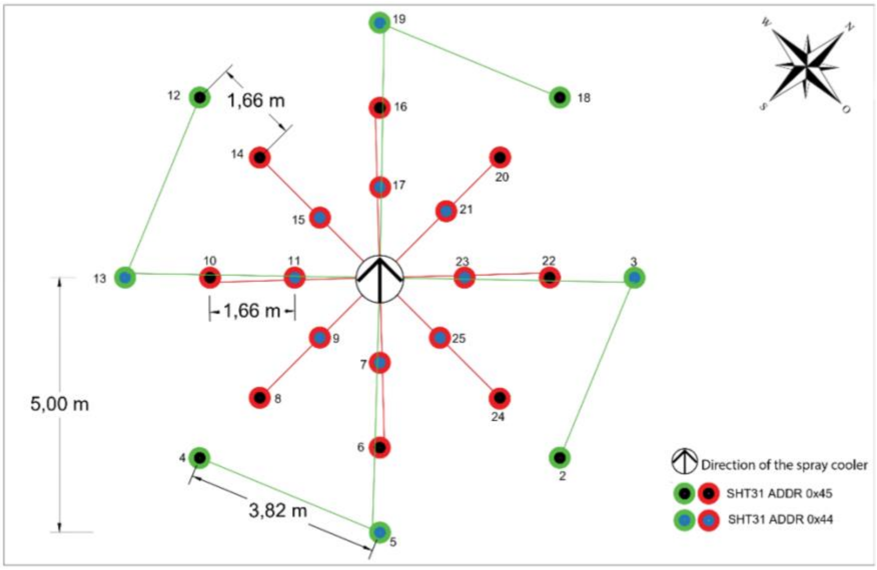

Figure 7. Radial arrangement of 24 SHT31 sensors, from Authors (2025)

Supporting structure for 24 SHT31 sensors distributed radially consisted of eight pairs of metal supports fixed to the ground. Between each pair of supports along a radial line, a smooth wire was stretched to serve as a support for attaching the sensors. On each of the eight radial lines, three SHT31 sensors were fixed to the wire, maintaining an even spacing of approximately 1.66 meters between them and positioned at a height of 1.65 meters. Figure 8 shows the complete field installation. The reference SHT31 sensor (index 1) was installed on a ninth similar metal support, positioned about 10 meters from the sprayer.

Figure 8. Installation of the measurement and cooling systems, from Authors (2025)

3. RESULTS AND DISCUSSION

This section presents the results obtained during one day of measurement (February 21), with the water spray cooling system operating continuously from 09:00 to 16:00. The analysis focused on the variation of temperature and humidity measured by the SHT31 sensors over time, environmental conditions (wind), and the system's operating pressure.

Sensor data was received with latencies often below 10 seconds, as illustrated in Figure 9. Although most transmissions occurred without issues, sensors experienced occasional interference, resulting in null readings for temperature and humidity. Voltage analyses on the 5V line revealed sudden drops in the logic level of the power supply voltage to the ESP32 and the connected sensors, which may have caused these temporary failures.

B	C	D	AU	AV	AW	AX	AY	AZ	BC	BD	BE
	Sensor 1 (reference)		Sensor 23		Sensor 24		Sensor 25				
Times	Temperature	Humidity	Temperature	Humidity	Temperature	Humidity	Temperature	Humidity	Pressure	Speed	Direction °
09:06:06	33,57	43,83	33,94	41,00	33,35	42,06	33,87	39,69	91,65	1,48	225
09:06:16	33,54	43,89	33,94	40,95	33,38	42,02	33,85	39,70	88,54	1,52	0
09:06:26	33,57	43,68	33,96	41,02	33,42	41,85	33,88	39,60	92,20	0,81	270
09:06:38	33,57	43,66	33,97	40,86	33,45	41,76	33,88	39,46	92,38	0,97	270
09:06:43	33,60	43,66	33,94	40,90	33,43	41,79	33,88	39,51	15,00	0,78	315
09:06:53	33,60	43,63	33,96	40,87	33,51	41,72	33,87	39,53	92,38	1,33	270

Figure 9. Data from all 28 sensors received in a Google Sheets spreadsheet, from Authors (2025)

After excluding null data, temperature variation was observed in the morning at the sensor positioned outside the system's influence area (ambient reference), ranging from 34.72 °C to 42.54 °C (Figure 10). During the afternoon period, the ambient temperatures were even higher, varying from 40.87 °C to 46.14 °C. Consequently, the relative humidity values were lower (Figure 11), ranging between 42.38% and 28.30% in the morning, and between 30.98% and 22.42% in the afternoon at sensor 1 (also outside the spray zone).

The sensors that recorded the greatest temperature reductions were those closest to the cooling system, notably sensors 15 and 17. Sensor 17, positioned ahead of the spray direction, showed the lowest temperatures: between 30.51 °C and 36.69 °C in the morning, and between 34.35 °C and 40.42 °C in the afternoon. Regarding humidity, this sensor also recorded the highest values, varying from 61.78% to 38.54% in the morning, and from 48.61% to 27.66% in the afternoon. Visual analysis of temperature gradients around the system is essential to quantify the thermal reduction and delineate the cooling effect area.

The data visually indicates a trend of lower temperatures near the spray system, demonstrating its cooling effect. It is important to highlight that sensor 3 showed readings influenced by the shadow of a nearby tent during the early morning hours, which may have caused locally lower temperatures not directly attributable to the cooling system.

Even under conditions of high thermal stress and humidity, which could compromise reading accuracy, the SHT31 sensors demonstrated the ability to capture small variations in temperature and humidity caused by passing clouds and oscillations in the spray direction. This suggests that neither the thermal shield nor the enclosures significantly interfered with data quality.

Thus, there is a visible trend of lower temperatures near the spray system, indicating the cooling effect. It is important to note that sensor 3 had readings influenced by the shadow of a nearby tent during the early morning, which may have resulted in locally lower temperatures not directly attributable to the cooling system.

Even under these conditions of higher thermal stress and excessive humidity, which could cause wetting and erroneous data, the SHT31 sensors were able to capture small variations in temperature and humidity related to temporary clouds and changes in the direction of the water spray, indicating that neither the thermal shield nor the enclosures interfered with data acquisition.

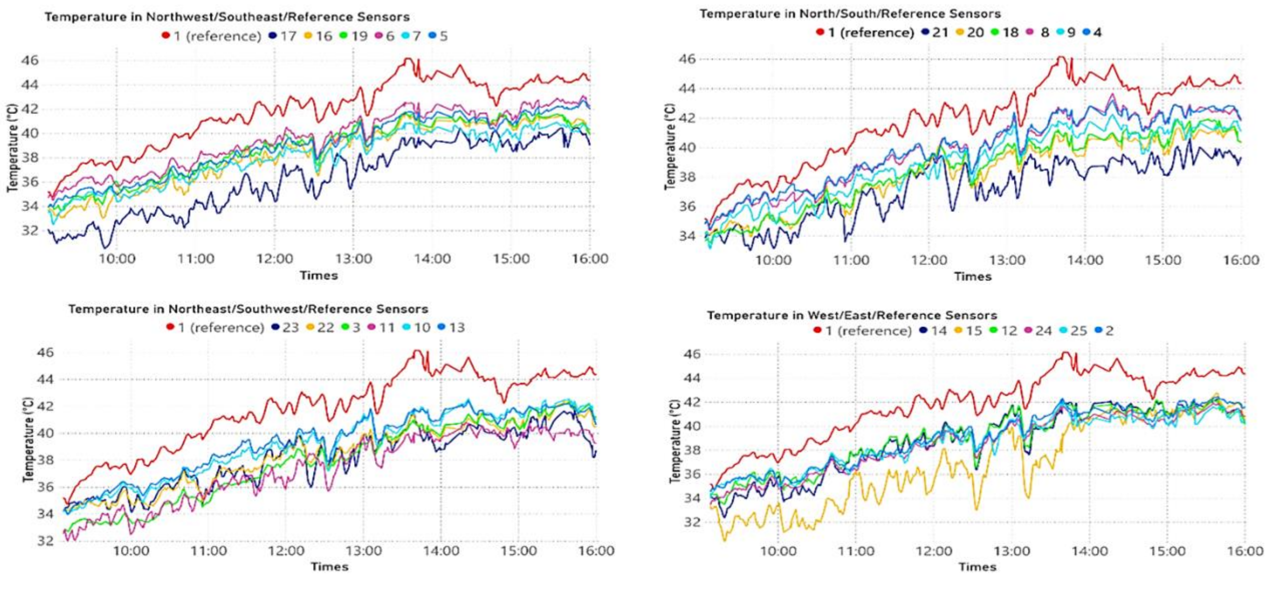

Figure 10. Temperature records from 25 SHT31 sensors during one day with the cooling system turned on, from Authors (2025)

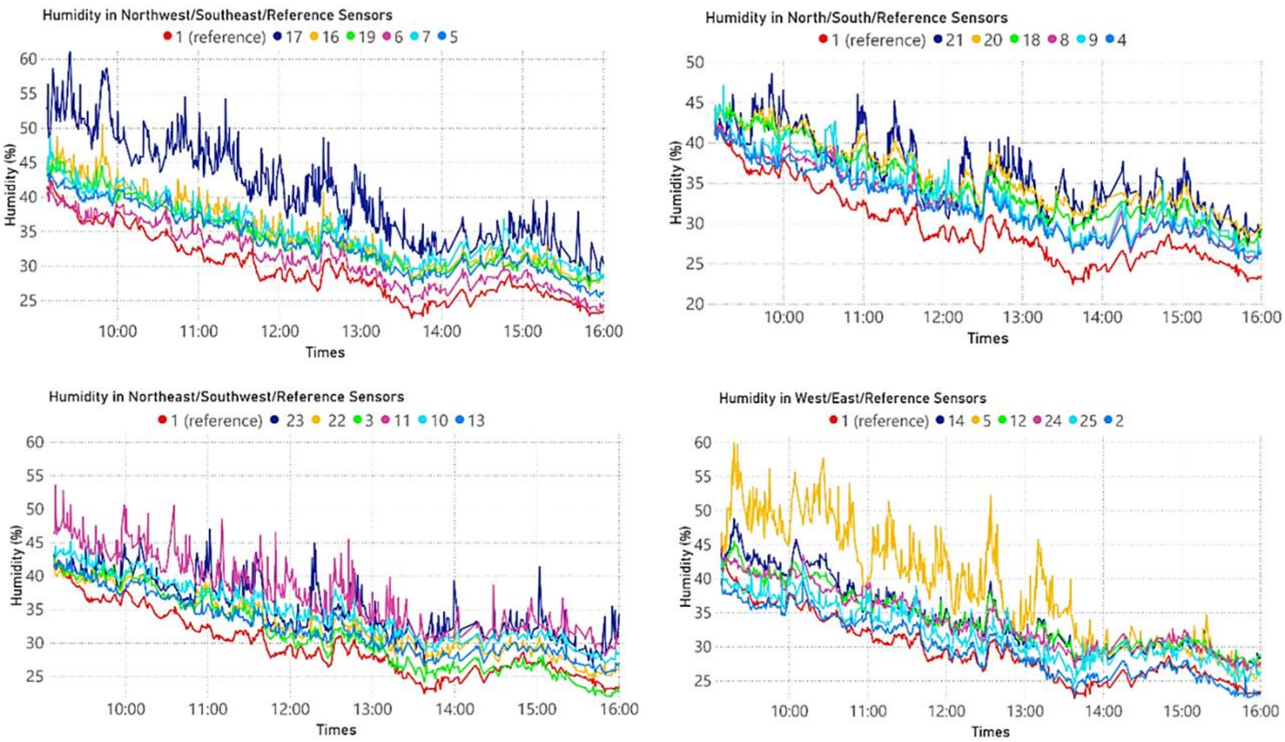

Figure 11. Humidity records from the 25 SHT31 sensors during one day with the cooling system turned on, from Authors (2025)

The pressure transmitter recorded a variable pressure ranging from 551 to 689 kPa, highlighting the cooling system as one close to a low-pressure system. According to Li and Willits (2008), they describe that high-pressure spray systems operate at compression of 6.89 MPa, while low-pressure spray systems operate at 405 kPa.

The direction sensor was fundamental for understanding the dispersion patterns of cooled air and water droplets from the system. The analysis of wind directions in the morning shows that the predominant wind directions were East (22.94%), Northeast (20.57%), Southeast (16.08%), and North (13.96%). This indicates that the air cooled by the spray system would tend to be dispersed toward the West, Southwest, and South regions of the sensor arrangement, depending on the interaction with wind speed.

In the afternoon period, the predominant wind directions were Southeast (21.28%), South (13.59%), East (13.45%), and Northeast (13.04%). Compared to the morning, the distribution of wind directions in the afternoon was more dispersed, although Southeast was still prominent. The wind speed sensor indicated wind speeds above 0.78 m/s, reaching up to 5.63 m/s, with an average speed of 1.03 m/s.

4. CONCLUSION

Despite occasional interference in SHT31 data, constructed data acquisition system demonstrated good stability and sensitivity, even under conditions of high humidity and heat. The measurement system, combined with more measurements and statistical analyses of the data obtained, can indicate that evaporative cooling is a viable alternative to mitigate thermal discomfort in outdoor spaces.

Temperature difference between ambient and cooling area indicated a maximum of 6,18 °C in the morning and with temperatures collected at 1.66 meters from the climatization system. In terms of air humidity, a maximum of 61.78% was observed during the morning which represented an increase of almost 19% from reference ambience.

5. ACKNOWLEDGEMENTS

The authors thank Universidade Federal do Oeste da Bahia (UFOB) for providing infrastructure resources for this research.

6. REFERENCES

Albuquerque, A.C.S.; da Silva, A.G. "Clima do bioma Cerrado", https://www.researchgate.net/publication/301567134_Clima_do_Bioma_Cerrado.pdf. Accessed in: 3 nov. 2024.

Cornei, D.; Fosalau, C.; Cornei, L., 2024. "A Cheap and Practical IoT Solution for Agricultural Data Monitoring". In *EPEi 2024 - Proceedings of the 2024 13th IEEE International Conference and Expositions on Electric and Power Engineering*, pp. 47–52.

da Cunha, A.R., 2015 "Evaluation of measurement errors of temperature and relative humidity from HOBO data logger under different conditions of exposure to solar radiation". *Environmental Monitoring and Assessment*, Vol. 187, n. 5, pp. 1–11.

Deshmukh, P.; Pawar, G.; Deshmukh, N.; Garde, C.; Deshmukh, M.; Raut, K., 2023. "Development of Low-Cost Temperature and Relative Humidity Remote Monitoring System". In *2023 IEEE Region 10 Symposium, TENSYMP 2023*.

IBGE. "Mapa de clima do Brasil". Instituto Brasileiro de Geografia e Estatística, Rio de Janeiro, https://www.ibge.gov.br/geociencias/cartas-e-mapas/informacoes-ambientais/15817-clima.html?edicao=15887&t=acesso-ao-produto. Accessed in: 4 nov. 2024.

Texas Instruments. "PCA9548A Low Voltage 8-Channel I 2 C Switch with Reset", https://www.ti.com/lit/ds/symlink/pca9548a.pdf?ts=1746580515951. Accessed in: 23 jan. 2025.

Li, S.; Willits, D.H., 2008 "Comparing low-pressure and high-pressure fogging systems in naturally ventilated greenhouses". *Biosystems Engineering*, Vol. 101, n. 1, pp. 69–77.

Measnet. "Anemometer Calibration Procedure", MEASNET, UPM, Madrid, Spain, https://www.measnet.com/wp-content/uploads/2011/06/measnet_anemometer_calibration_v2_oct_2009.pdf. Accessed in: 4 jun. 2025.

Camargo, J. R., 2003. "Sistemas de resfriamento evaporativo e evaporativo-adsortivo aplicados ao condicionamento de ar", Phd Thesis, Universidade Estadual Paulista, Guaratinguetá, p. 140.

Sensirion. Datasheet SHT3x-DIS, Sensirion The Sensor Company, https://sensirion.com/media/documents/213E6A3B/63A5A569/Datasheet_SHT3x_DIS.pdf. Accessed in: 23 jan. 2025.

Sunny, A.I.; Zhao, A.; Li, L.; Sakiliba, S.K, 2020. "Low-Cost IoT-Based Sensor System: A Case Study on Harsh Environmental Monitoring". *Sensors*, Vol. 21, Page 214.

7. RESPONSIBILITY NOTICE

The authors are the only responsible for the printed material included in this paper.